An electrostatic charge repulsion algorithm for dynamic ordering of 3D projections

Gregory R. Lee[1,2], and Mark A. Griswold[1,2]

[1]*Radiology, Case Western Reserve University, Cleveland, OH, United States,* [2]*University Hospitals Case Medical Center, Cleveland, OH, United States*

Introduction

For increased flexibility in dynamic imaging applications it is desirable to order the individual projections of a 3D radial acquisition so that they are approximately equally distributed over k-space at any time scale. The 3D golden means algorithm [1] is applicable in cases where a single, linear projection is acquired per TR (Fig. 1a,b) so that the orientation is fully defined by a set of 2 angles. The algorithm is not applicable to more general cases, such as bent projection imaging (Fig. 1c) or cases where multiple projections are acquired in a single shot (Fig. 1d). In these cases, an additional rotation angle is required to fully define the orientation. In this work, the authors propose a new algorithm that is applicable to all cases shown in Fig. 1. The algorithm is an extension of previously proposed numerical methods for calculating optimal packing of charges on the surface of a sphere [2,3]. Charge repulsion algorithms start with an arbitrary configuration of charges and obtain a minimal potential energy iteratively via descent.

Theory

Let the endpoint of each projection be treated as a point charge. Rather than allowing each point charge to move independently as in [2,3], we fix the relative locations of the charges within a single shot to preserve its shape. Each shot is treated as a rigid body with axis of ration at the origin. A net force at each "charge" is calculated as the sum of the Coulomb forces from all charges in all other shots (charges within a given shot do not exert a force on each other). Specifically, the net Coulomb force, $\vec{F}_{i,k}$, on a charge, k, within shot i is given by Eq. 1:

$$\vec{F}_{i,k} \propto \sum_{\substack{s=1 \\ s\neq i}}^{N_s} \sum_{p=1}^{N_p} \frac{\vec{r}_{i,k}-\vec{r}_{s,p}}{|\vec{r}_{i,k}-\vec{r}_{s,p}|^3} \quad [1], \qquad \vec{\tau}_{i,k} = \vec{r}_{i,k} \times \vec{F}_{i,k} \quad [2], \qquad \vec{\tau}_i = \sum_{k=1}^{N_p} \vec{\tau}_{i,k} \quad [3], \qquad \vec{F}_{i,k} \propto \sum_{\substack{s=1 \\ s\neq i}}^{N_s} \sum_{p=1}^{N_p} \frac{(\vec{r}_{i,k}-\vec{r}_{s,p})}{\Delta t_{i,s}^{\beta}|\vec{r}_{i,k}-\vec{r}_{s,p}|^3} \quad [4]$$

where N_s is the total number of shots, N_p is the number of projections within a single shot, and $\vec{r}_{i,k}$ is the spatial position of charge k within shot i. The net force on each charge within a given shot contributes a torque, $\vec{\tau}_{i,k}$ (Eq. 2). The net torque,$\vec{\tau}_i$, on shot i is simply a sum over the torques applied to all charges within that shot (Eq. 3). Once the net torque has been computed for a given shot, an axis of rotation is defined as $\vec{u}_i = \vec{\tau}_i/|\vec{\tau}_i|$ and a rotation angle about this axis is calculated as $\varphi_i = \alpha|\vec{\tau}_i|$ to give a rotation matrix, R_i. The position of each charge is then updated as $\vec{r}_{i,k} = R_i \vec{r}_{i,k}$. α is a scaling factor set small enough that the new positions reduce $\vec{F}_{i,k}$ in the following iteration. To improve the spatial distribution at a variety of timescales, Eq.1 can be replaced by Eq. 4 where $\Delta t_{i,s}$ is the magnitude of the temporal distance between shot i and shot s. $\beta \geq 0$ is a constant. This temporal term results in the forces being scaled up for shots that are close together in time. Larger values of β optimize the spatial distribution at short timescales at the cost of less equidistant samples over longer timescales. Setting β to zero is equivalent to Eq. 1 (no temporal penalty).

Methods

The proposed algorithm was run for the case of Fig. 1b with 512 shots (N_p=2, N_s=512). The algorithm was also run for the more demanding case of Fig. 1d with 4096 multiecho shots (N_p=10, N_s=4096). The algorithm was initialized using randomized orientations for each shot. β was initialized to 4 and then was decreased by 0.02 after every 40 iterations to encourage even distribution of samples at all time scales. The algorithm was stopped after β=0.

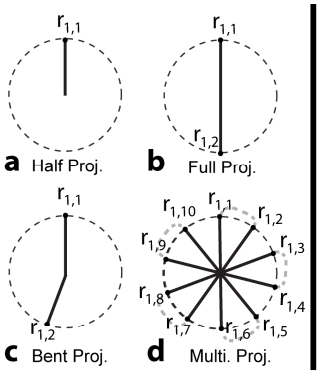

Fig. 1: Trajectory cases

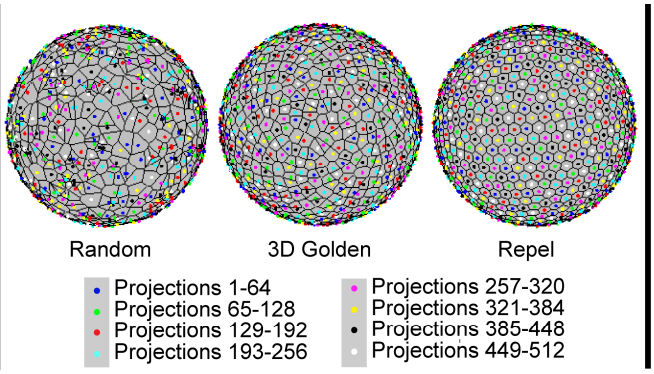

Fig. 2: Comparison of projection locations after 512 shots.

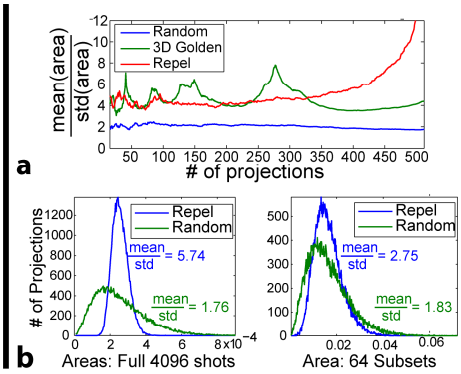

Fig. 3: a) 512 shot, Full Proj. b) 4096 shot,Multi Proj.

Results and Discussion

Fig. 2 shows projection locations (dots) and each corresponding Voronoi cell (solid lines) for the trajectory of Fig. 1b. with 512 total shots. Subsets of the full number of projections are indicated by different colors. The full set of samples is most uniformly distributed for the charge repulsion algorithm. Fig. 3a plots the mean over standard deviation of the Voronoi cell areas at all subets of the full number of shots. The larger the y-axis value, the more uniform the sampling pattern is over the corresponding time scale. It can be seen that the repel algorithm is by far the best over the full set of projections, although it is outperformed by the 3D Golden angle approach for some specific subsets of the full number of shots. Fig. 3b plots histograms of the Voronoi cell areas over the full set of 4096 shots (left) and for all subsets of 64 shots (right) of the multiecho trajectory (Fig. 1d). The improvement over random sampling is clearly indicated by the narrow distribution of areas. The 3D Golden angle approach is not applicable in this case. In summary, the proposed algorithm provides a large improvement over randomized sampling at all time scales for all 3D radial acquisition types.

References: 1. Chan et al. MRM 2009;61(2):p.354. 2. Cohn, H. MTAC 1956;10(55):p.117. 3. Saff et al. The Mathematical Intelligencer 1997;19(1):p.5.

Support: This work was supported in part by Siemens Medical Solutions, as well as NIH 1RO1HL094557